

EARLY ONLINE RELEASE

This is a PDF of a manuscript that has been peer-reviewed and accepted for publication. As the article has not yet been formatted, copy edited or proofread, the final published version may be different from the early online release.

This pre-publication manuscript may be downloaded, distributed and used under the provisions of the Creative Commons Attribution 4.0 International (CC BY 4.0) license. It may be cited using the DOI below.

The DOI for this manuscript is

DOI:10.2151/jmsj.2021-036

J-STAGE Advance published date: March 12th, 2021

The final manuscript after publication will replace the preliminary version at the above DOI once it is available.

1
2
3
4
5
6
7
8
9
10
11
12
13
14
15
16
17
18
19
20
21
22
23
24
25
26
27
28
29

**An efficient practical post-processing algorithm for the
quality control of dual-pulse repetition frequency
Doppler velocity data**

Yoshinori YAMADA¹

Meteorological Research Institute, Japan Meteorological Agency, Tsukuba, Ibaraki, Japan

March 30, 2020

Revised: 23 November, 2020

Revised: 11 December, 2020

Revised: 8 February, 2021

1) Corresponding author: Yoshinori Yamada, Meteorological Research Institute, Japan
Meteorological Agency, 1-1, Nagamine, Tsukuba 305-0052 JAPAN.
Email: yyamada@mri-jma.go.jp
Tel: +81-29-853-8643

30 Fax: +81-29-853-8649

31

32

Abstract

33

34 This paper presents an efficient, practical post-processing algorithm for the quality
35 control of dual-pulse repetition frequency (dual-PRF) Doppler velocity data observed in
36 Plan Position Indicator (PPI) mode. Quality control refers to the enhancement of the
37 quality of the Doppler velocities through the re-assignment of an appropriate Nyquist
38 interval number to an erroneous velocity datum and the elimination of unreliable data.
39 The proposed algorithm relies on the local continuity of velocity data, as do most of the
40 preexisting algorithms. Its uniqueness, however, lies both in the preparation of more
41 reliable reference velocity data and its applicability to PPI data at higher elevation angles.
42 The performance of the proposed algorithm is highlighted by its application to observed
43 data from C- and X-band Doppler radars. This algorithm is practical, efficient, and not
44 time consuming. It may be of great help in the derivation of accurate wind information
45 from dual-PRF Doppler velocities.

46

47 **Keywords** Doppler velocity; quality control; dual-PRF

48

49 1. Introduction

50 Doppler radars provide valuable wind information at high temporal and spatial resolutions
51 in operational and research fields. Pulsed Doppler radars have, however, a limitation
52 resulting from the existence of the unambiguously measurable maximum velocity, called the
53 Nyquist velocity v_a . This velocity is given as

$$54 v_a = \lambda \cdot PRF/4,$$

55 where λ is the transmitted wavelength, and PRF is the pulse repetition frequency. The
56 measured Doppler velocities are then ambiguous by $2n v_a$, where n is an integer called the
57 Nyquist interval number. Due to the so-called Doppler dilemma, most pulsed Doppler
58 radars are operated around v_a in the range of 10–20 m s⁻¹ to ensure a sufficient detection
59 range. For such values of v_a , the measured Doppler wind fields are often contaminated
60 by folding or aliasing. An appropriate Nyquist interval number n should thus be assigned
61 to each velocity datum before analyzing Doppler velocities.

62 Folding effects can be alleviated through the use of the dual-PRF (dual-pulse repetition
63 frequency) technique (e.g., Diviak and Zrnić 1993), which extends the unambiguous velocity
64 interval. A practical implementation of this technique for Plan Position Indicator (PPI)
65 scanning is to collect velocity data by a beam-by-beam alternation of two PRFs during
66 antenna rotation, assuming that the same space is probed at two different PRFs
67 simultaneously. The dual-PRF method is now commonly used for operational Doppler
68 radars, including the C-band Doppler radars operated by the Japan Meteorological Agency

69 (abbreviated as JMA) (Tsukamoto et al. 2016) and the X-band multi-parameter Doppler
70 radars deployed by the Ministry of Land, Infrastructure, Transport, and Tourism (abbreviated
71 as MLIT) (Maesaka et al. 2011).

72 Doppler velocities from the dual-PRF technique are not, however, free from dealiasing
73 errors and/or statistical (random) errors. Thus, post-processing algorithms have been
74 developed (e.g., Holleman and Beekhus 2003; Joe and May 2003; Altube et al. 2017).
75 Hereafter, the algorithm developed by Holleman and Beekhus is denoted as HB03, the
76 algorithm by Joe and May is called JM03, and the algorithm by Altube et al. is called AL17.
77 These three algorithms are all based on the local continuity of Doppler velocities collected
78 in PPI mode. HB03 uses a median velocity as a reference, computed in a window centered
79 at the target point being considered, while JM03 employs the Laplacian operator for the
80 detection and correction of erroneous data. In contrast to these two methods, AL17
81 processes the correction in the phase space instead of the velocity space. These three
82 algorithms have shown good performance in correcting dual-PRF velocity errors in PPI
83 scans at low elevation angles less than 10 degrees. It is nevertheless very difficult to
84 perfectly correct all errors in the velocity data. Furthermore, it is also not clear how these
85 three methods function for velocity data in PPI scans at higher elevation angles of about 20–
86 40 degrees, which are commonly employed in VAD analysis (Browning and Wexler 1968)
87 and multiple-Doppler wind synthesis. No concrete theories or perfect methods exist for the
88 correction of dual-PRF velocity errors up to the present date. It is therefore worth

89 developing efficient and high-performance algorithms for the correction of the errors in the
90 dual-PRF velocities that are applicable to Doppler velocities collected in PPI, which is
91 currently a major observation mode, to facilitate deriving reliable wind information.

92 This paper presents an efficient, practical post-processing method for the quality control
93 of dual-PRF Doppler velocity data in PPI mode, regardless of the cause of the errors.
94 Quality control refers to an overall process used to enhance the quality of Doppler velocities
95 by the re-assignment of an appropriate Nyquist interval number to an erroneous datum and
96 the elimination of false data. The proposed algorithm, processed in velocity space, relies
97 on local continuity, as do HB03, JM03, and AL17. Its uniqueness, however, lies both in the
98 preparation of the reference data and its applicability to PPI data at higher elevation angles.
99 Section 2 will describe the principle of the quality control, followed by an application of the
100 method to observed data in Section 3. A discussion of the results is presented in Section
101 4, and conclusions are given in Section 5.

102

103 2. Principle of quality control

104 The principle of the proposed algorithm is based on the combination of a gap check and
105 a subsequent correction at each range gate with an observed datum. This combination is
106 applied to each of the observed data in a PPI scan of interest, and the processing of all of
107 the data of concern in the scan will be repeated for several cycles until the unreliable data
108 and/or errors are completely corrected or removed. A flowchart of this algorithm is shown

109 in Fig. 1, in which the symbols in parentheses indicate important processes that are
110 referred to in the text. Without the presence of extended Nyquist aliasing, the algorithm
111 requires no supplementary wind information. Prior to the application of this algorithm, it is
112 assumed that classical quality control, based on reflectivity and/or Doppler width
113 thresholds (for example), is performed. This paper does not refer to the quality control
114 measures for meteorologically-unimportant velocity data, such as those that have been
115 severely contaminated by ground clutter and those caused by radio wave interference.

116  Fig. 1

117 2.1 Gap check step

118 The algorithm starts from the gap check at every range gate with an observed datum.
119 This step is conducted to detect the existence of “unnaturally” large gaps in the velocity field
120 in a PPI scan of interest because such large gaps are mostly associated with erroneous
121 and/or false data. The gap check step in the first round is, however, not accompanied by
122 the correction step (G-10) because of a lack of the necessary parameters for correction.

123 To detect large discontinuities at each range gate, the deviations of the datum considered
124 in terms of nearby velocities are investigated. For this purpose, we define a small region,
125 or window, which is centered at each range gate (G-1), as in HB03 and JM03. When the
126 window contains at least a minimum number of observed data (denoted as N_0) (G-2), the
127 detection of large gaps is processed in this window through examining the deviations
128 (denoted as δV_r) of all velocities from the datum located at its center (G-3). If the number

129 of data is less than N_0 , the processing moves to the gap check at the next range gate. The
130 $|\delta V_r|$ larger (equal to or smaller) than a prescribed threshold value (denoted as δ_1) is
131 regarded as a large (small) gap. During this gap check, a datum with a small gap is marked
132 “without gap”, while a datum related to a large gap is labeled “with gap.” In addition, the
133 number of occurrences of “without gap” and “with gap” are counted separately. When no
134 large gaps are detected in the window being considered (G-4), this window is regarded as
135 being gap-free, and all data in this window are marked as “good” (G-5). Furthermore, a
136 mean Doppler velocity (denoted as V_m), defined at the center of this window, is computed
137 with all of the available data in the window using a distance-weighted averaging (G-6). The
138 weight has a form of $1/(1 + R^{1/2})$, where R is the distance from the range gate at the
139 center of the window, and is computed from the relative differences in gate and beam
140 numbers. This V_m may have a higher degree of reliability as a mean value near the target
141 range gate, as long as the dual-PRF technique functions properly, and it will be a candidate
142 for a reference value in the correction. No correction is made for this gap-free window, and
143 the gap check is resumed at the next range gate. In contrast, when at least one large gap
144 is detected in the window (G-3), this window is marked as “with-gap” (G-4), and all data in
145 the window are labeled as being “doubtful” (G-7). In addition, one of the following two
146 procedures is performed, depending on the number of occurrences of large gaps (G-8).

147 (1) When the ratio of the small gap occurrences to the total number of observed data is
148 larger than a prescribed threshold (denoted as R_0), a provisional mean velocity (denoted as

149 V_{pm}), defined at the center of the window, is computed (G-9) in a similar manner to G-6,
150 using only velocities marked “without gap.” This V_{pm} will be used to determine an
151 appropriate reference velocity among the V_m s nearby, computed from the gap-free windows.
152 The correction of doubtful data described in the next subsection is subsequently processed
153 for this with-gap window, as shown by a gray bold solid line in Fig. 1.

154 (2) Otherwise, no V_{pm} is computed for this window, and the processing immediately
155 returns to the gap check at the next range gate.

156

157 2.2 Correction step

158 When a with-gap window with V_{pm} is detected at a range gate under examination, the
159 correction of unreliable data is immediately made for this window from the second round on
160 (G-10). This procedure may enhance the performance of the proposed algorithm, because
161 the reduction in numbers of unreliable data instantly exerts a beneficial influence on the
162 processing of the remaining doubtful data. To correct “doubtful” velocities in this window,
163 a reliable reference velocity (denoted as V_{ref}) will be explored with the aid of V_{pm} . For this
164 purpose, we define another window of a certain size, centered at the target data point being
165 considered (C-1). A reliable reference value will then be selected among the V_m s
166 computed for the gap-free windows, whose centers are located in this window (defined in
167 C-1), such that the reference minimizes the magnitude of the deviation from V_{pm} (C-2). If
168 no such reference velocity exists (C-3), the processing quickly returns to the gap check step

169 at the next range gate, as indicated by a gray bold dotted line in Fig. 1. When such a
170 reference is found (C-3), V_{pm} is corrected with the local continuity using V_{ref} . If the
171 magnitude of the difference (denoted as δV_2) between the resultant corrected value and
172 V_{ref} is less than a threshold (denoted as δ_2 , which is given as αV_{ah} , where α is the same
173 value as in C-7, explained later, and V_{ah} is a higher Nyquist velocity, respectively) (C-4), the
174 V_{pm} at this range gate is replaced by V_{ref} , which is treated as the mean velocity from the
175 gap-free window (C-5).

176 The correction of all unreliable data in the window defined at this point is subsequently
177 made using the local continuity (C-6), employing V_{ref} as a reference. The quality of the
178 corrected datum is further checked by the method described in Yamada and Chong (1999)
179 (C-7). This check helps remove low-quality data that cannot be detected by the classical
180 tests, based on the thresholds of reflectivity and/or the Doppler widths. If the difference
181 (denoted as δV_3) between the corrected datum and V_{ref} falls within $\pm\alpha v_a$, where α (<
182 1) is a predetermined positive constant that should be appropriately set depending on the
183 case in question, the corrected datum is re-labeled as “good” (C-8). Values of α of
184 approximately 0.3 to 0.4 are commonly used. On the contrary, if δV_3 does not satisfy the
185 above condition, this datum is no correction is made, and the datum remains “doubtful” (C-
186 9). This correction processing is repeated for all doubtful data in the window of interest.

187 After the correction is completed for all doubtful data in the window being considered, the
188 processing returns to the gap check at the next range gate (C-10). Since the correction

189 step does not process “doubtful” velocity data at the range gates without V_{pm} , the above
190 point-by-point processing, based on the gap check and followed by the correction, will be
191 repeated several times for data in a PPI scan. If the number of iterations exceeds a
192 predetermined maximum count, all of the data that remain doubtful are finally deleted.

193 One advantage of the present algorithm, relative to HB03 and JM03, is the determination
194 of a more reliable reference velocity through a combination of the corresponding provisional
195 mean velocity and the mean velocities computed for the gap-free windows neighboring the
196 target point. HB03 and JM03 make the correction by using data that is, principally, in a
197 window of small size, e.g., 3 x 3 points, centered at the range gate. The resultant small
198 number of data would cause a performance degradation in their algorithms in the presence
199 of relatively high contamination by noise and/or erroneous data, for example. In contrast,
200 the proposed algorithm determines a reference value among the mean velocities computed
201 for the respective gap-free window, whose center is inside the window defined in C-1.
202 Since this reference has the mean character of a chunk of “smoothed” velocities existing
203 near the target grid point, it will be more suitable and reliable for correcting the doubtful
204 datum at the range gate considered.

205

206 **3. Application of the proposed algorithm to observed velocity data**

207 This section will demonstrate the performance of the proposed algorithm through its
208 application to observed dual-PRF velocities in PPI mode for three cases. Two of the cases

209 are for data from C-band Doppler radars operated by JMA, and the other is for data from an
210 X-band Doppler radar operated by MLIT. For the three cases, the reflectivity threshold of
211 10 dBZ was applied to the Doppler velocities to remove undesirable data before the quality
212 control using the proposed algorithm is made.

213 The first example is a correction of velocity data from a C-band Doppler radar operated
214 at Tokyo International Airport (Haneda Airport) for a case of heavy local rainfall in central
215 Tokyo on September 4th, 2005. This radar is located at 139.7561°E and 35.5561°N and
216 was operated at two PRFs of 840 Hz and 1120 Hz, corresponding to Nyquist velocities of
217 11.92 m s⁻¹ and 15.90 m s⁻¹, respectively. The extended Nyquist velocity thus becomes
218 47.7 m s⁻¹. The radar collects data with spatial resolutions from 0.15 km up to 128 km in
219 the radial direction and 0.7° in the azimuthal direction. The numbers of the beam and gate
220 are 512 and 800, respectively.

Fig. 2

221 Figure 2a shows an observed Doppler velocity in a PPI scan at an elevation angle of 2.1°
222 at 2307 JST¹. Contamination by errors and/or noises spreading across the data is easily
223 identified in this figure. When the present algorithm is applied, the size of the window for
224 the gap check defined at each range gate is 7 points in the azimuthal direction and 7 points
225 in the radial direction. The gap check process is performed for the window that contains
226 the number of observed data equal to or larger than 12, that is, $N_0 = 12$. The threshold of
227 the velocity difference (δ_1) for the gap detection was set to 18 ms⁻¹. Such a large value helps

¹ JST: Japan Standard Time. JST = UTC + 9 hours.

228 us to detect erroneous data without confusing it for “real” gaps in Doppler velocities.

229 The provisional mean velocity is computed in each window when R_0 is equal to or larger
230 than 0.9 and 0.75, respectively, for the first gap check and afterwards. The more severe
231 condition imposed on the first gap detection step is to prepare more reliable reference
232 velocities. To correct velocity data labeled “doubtful” in the subsequent correction step, an
233 appropriate reference velocity is selected in a window of the same size (C-1) for the gap
234 check process (G-1).

235 The corrected velocity field in Fig. 2b was finally obtained through four cycles of the
236 combination of the gap check and correction steps for this case. In the correction step,
237 $\alpha = 0.45$ was employed for the quality of the corrected datum in C-7. Using the same
238 value of α , δ_2 is set equal to αV_{ah} . The quality of the velocities in this figure is excellent.
239 In addition, a comparison of Figs. 2a and 2b indicates that the “good” data remain unaffected
240 during quality control processing. This is a common feature of the cases illustrated in Figs.
241 3 and 4. The respective values of N_0 , δ_1 , R_0 , and α as well as the determination of δ_2
242 for this example are also employed in the following two examples. Additionally, the same
243 size of the window for the gap check (G-1) and the determination of a reference velocity (C-
244 1) are used.

Fig. 3

245 The second example is a correction of data from a JMA C-band Doppler radar (located at
246 141.6767°E and 42.7961°N), operated at the New Chitose Airport (CTS) in Hokkaido, Japan.
247 This example will also demonstrate that the proposed algorithm has the potential to correct

248 data with a relatively high degree of contamination by unreliable data in a PPI scan, even at
249 higher elevation angles. The spatial resolutions of this radar and the two PRFs are the
250 same, respectively, as in Fig. 2. The high and low PRFs correspond to Nyquist velocities
251 of 15.90 m s^{-1} and 11.92 m s^{-1} , respectively, and the extended Nyquist velocity is then 47.7
252 m s^{-1} . Figure 3a displays velocity data in PPI at an elevation angle of 32.1° , collected for
253 a precipitation system producing heavy rainfall on August 27th, 2013 in and around the city
254 of Tomakomai, located to the south-southwest of CTS at a distance of about 15 km. The
255 readily discernible false data, or outliers, are scattered in a wider area. The cause of such
256 erroneous data is unclear. After the gap check and correction steps were repeated four
257 times, the quality of the Doppler velocities is successfully refined, as shown in Fig. 3b.

Fig. 4

258 The final example is an application to data from an X-band Doppler radar of the Ushio site
259 (located at 132.5500°E and 34.5050°N), part of the Extended Radar Information Network
260 (called XRAIN) operated by MLIT. The maximum detection range of this radar is 80 km,
261 and the numbers of the gate and beams are 534 and 300, respectively. Its spatial
262 resolution is 0.15 km in the radial direction and 1.2° in the azimuthal direction. The PRFs
263 of this radar are 1500 Hz and 1200 Hz, corresponding to Nyquist velocities of 11.54 m s^{-1}
264 and 9.24 m s^{-1} , respectively. The extended unambiguous maximum velocity is then 46.2
265 ms^{-1} . Figure 4a shows velocity data in PPI at an elevation angle of 4.9° . This data was
266 associated with a precipitation system producing torrential rainfall in Hiroshima Prefecture
267 on July 6th, 2018. Erroneous velocity data are identified in the regions enclosed by yellow

268 lines. Figure 4b depicts an enlarged view of the portion indicated in Fig. 4a and also
269 represents the size of the window used in the gap check step relative to the areal extent of
270 erroneous data. Four cycles of the gap check and correction steps successfully completed
271 the quality control of the Doppler velocities as displayed in Fig. 4c. Figure 4d shows the
272 velocity field in Fig. 4b after correction, emphasizing the performance of the proposed
273 method for correcting errors located at and around the boundary of echoes.

274

275 4. Discussions

276 The algorithm proposed in the paper is based on the combination of the detection of
277 “unnatural” gaps and the subsequent correction step relying on the local continuity, as in
278 HB03 and JM03. Unlike the algorithms in these studies, the present algorithm is designed
279 to select a more reliable reference velocity among the mean velocities computed for the
280 surrounding gap-free windows close to the range gate considered, for which a provisional
281 mean velocity is computed. This process enhances the performance of the algorithm by
282 using a more suitable reference value and may correct even velocity data contaminated by
283 a relatively large number of erroneous velocities, as shown in Figs. 2a and 3a. In addition,
284 the advantage of the present method is its applicability to data in PPI at higher elevation
285 angles. Most previous studies did not address this point. Several repetitions of gap check
286 and correction cycles are sufficient for quality control.

287 HB03 and JM03 are based on the median velocity and the Laplacian operator, respectively.

288 The use of a median velocity in the window as a reference appeared to be insufficient
289 because the median value may be susceptible to the presence of unreliable data. Indeed,
290 when applied to data contaminated by a relatively large number of erroneous data in Fig.
291 3a, the proposed method did not give a satisfactory result when the median velocity was
292 chosen as a reference. The basis of JM03 is the modified Laplacian discrimination
293 parameter, which is given as a weighted summation of Doppler velocities in a window of size
294 3 x 3 points centered at the range gate being considered. This method appears to have
295 difficulty detecting and correcting errors if inappropriate Nyquist interval numbers are
296 assigned to all observed data of similar values in this window.

297 The size of the window in the radial direction should be adjusted when the method is
298 applied to PPI data at higher elevation angles under high vertical shear conditions. High
299 vertical shear may result in large differences in velocities in the window considered, so that
300 it is possible that the algorithm may regard such "natural" gaps as errors.

301 The method introduced in this paper can also be applied to velocity data without PRF
302 information in the recorded data, as in HB03 and JM03. In this case, the correction was
303 first made using each of the Nyquist velocities corresponding to high/low PRFs to compute
304 the respective tentatively corrected values. Then, an appropriate corrected datum will be
305 a datum that has a smaller deviation from the reference. The resultant corrected velocity
306 is, of course, checked for its appropriateness.

307 The performance of the method presented in this paper is highlighted in the three

308 examples, two of which are highly contaminated cases. It has, however, the following three
309 limitations, similar to the preexisting methods. First, there is a difficulty in correcting an
310 isolated cluster of erroneous data, regardless of their size, because large gradients are
311 hardly detected there. If its areal extent is small, such data would be meteorologically
312 unimportant. Next, there is a difficulty in the correction of a clump of embedded false data
313 that has a horizontal extent much wider than the window size employed. Such data would,
314 however, be rare, so long as the dual-PRF technique is functioning properly, except for cases
315 of very strong typhoon-associated winds exceeding the extended Nyquist velocity, for
316 example. The last limitation is the correction of velocities corresponding to the wind
317 components falling outside the extended unambiguous velocity interval. The present
318 method requires other techniques for global dealiasing prior to its application for such a case,
319 as do HB03 and JM03.

320 Regardless of these limitations, the proposed algorithm is found to perform well without
321 any subsidiary wind information. Furthermore, the algorithm is not time consuming. It
322 serves as a practically useful and efficient tool for the quality control of dual-PRF Doppler
323 velocity data, contributing to the extraction of accurate wind information.

324

325 **5. Conclusions**

326 This paper has presented a practical, efficient post-processing algorithm for the quality
327 control of dual-PRF Doppler velocity data collected in PPI mode and demonstrated its high

328 performance through its application to observed data, even to PPI data collected at higher
329 elevation angles and contaminated by a relatively large number of errors. The algorithm is
330 composed of a combination of the gap detection step and the following correction step.
331 The principle of the algorithm is based on the local continuity of Doppler velocities, like most
332 of the existing methods. The uniqueness of the proposed method lies in the preparation
333 and the determination of a reference velocity for correction and its applicability to data
334 collected in PPI scans at higher elevation angles. It requires no auxiliary wind information
335 in these steps, except for data contaminated by extended Nyquist aliasing. The repetition
336 of the above detection and correction steps several times will be sufficient to completely
337 remove unnatural gaps in velocity fields for most cases.

338 Since the algorithm is not time consuming, it is practically very useful for deriving accurate
339 wind information from dual-PRF Doppler velocities. In particular, it may be a valuable tool
340 for the accurate determination of three-dimensional wind fields from multiple-Doppler wind
341 synthesis, in which velocity data in many PPI scans from at least two Doppler radars should
342 be processed efficiently and accurately.

343 The algorithm has limitations, as do the preexisting methods. Since no methods exist at
344 present for the “perfect” quality control of dual-PRF Doppler velocities, it is still necessary
345 and worthwhile to elaborate efficient and high-performance methods to derive accurate wind
346 information from dual-PRF Doppler velocities.

347

348

Acknowledgments

349 The Doppler radar data from Tokyo International Airport (Haneda) and New Cjitose Airport
350 are provided by JMA. XRAIN datasets are provided by the Ministry of Land, Infrastructure,
351 Transport, and Tourism, Japan. The program “draft” is used to decode the JMA’s Doppler
352 radar data and the XRAIN data. This work was supported by JSPS KAKENHI Grant
353 Number JP26242036.

354 The author would like to thank two anonymous reviewers for their valuable comments for
355 improving this manuscript.

356

357

358

References

359

360

361 Altube, P., J. Bech, O. Argemi, T. Rigo, N. Pineda, S. Collis, and J. Helmus, 2017: Correction
362 of dual-PRF Doppler velocity outliers in the presence of aliasing. *J. Atmos. Oceanic*
363 *Technol.*, **34**, 1529-1543.

364 Browning, K. A. and R. Wexler, 1968: The Determination of Kinematic Properties of a Wind
365 Field Using Doppler Radar. *J. Appl. Meteor.*, **7**, 105–113.

366 Doviak, R. J. and D. S. Zrnić, 1993: *Doppler Radar and Weather Observations*, 2nd. Ed.,
367 Academic Press, 562 pp.

368 Holleman, I. and H. Beekhuis, 2003: Analysis and correction of dual PRF velocity data. *J.*
369 *Atmos. Oceanic Technol.*, **20**, 443-4453.

370 Joe, P. and P. T. May, 2003: Correction of Dual PRF Velocity Errors for Operational Doppler
371 Weather Radars. *J. Atmos. Oceanic Technol.*, **20**, 429-442.

372 Maesaka, T., M. Maki, K. Iwanami, S. Tsuchiya, K. Kieda, and A. Hoshi, 2011: Operational
373 Rainfall Estimation by X-band MP Radar Network in MLIT, Japan. *Preprints 35th Conf.*
374 *Conf. on Radar Meteorology*, Pittsburgh, PA., Amer. Meteor. Soc., P11.142.

375 Tsukamoto, N., H. Yamauchi, H. Okumura, A. Umehara and Y. Kajiwara, 2016: JMA's C-
376 band dual-polarization Doppler weather radars with SSPAs. *Technical Conference on*
377 *Meteorological and Environmental Instruments and Methods of Observation, 2016. World*
378 *Meteorological Organization*, P2(68), Madrid, Spain.

379 Yamada, Y. and M. Chong, 1999: VAD-based determination of the Nyquist Interval number
380 of Doppler velocity aliasing without wind information. *J. Meteor. Soc. Japan*, **77**, 447-
381 457.

382

383

List of Figures

384

385

386 Figure 1: Flowchart of the proposed algorithm. The symbols in parentheses indicate
387 important processes that are explained in the text.

388

389 Figure 2: (a) Beam-by-beam representation of Doppler velocity from the Haneda radar in a
390 PPI scan at an elevation angle of 2.1° . The abscissa indicates the beam number from
391 1 to 512 in a clockwise direction, corresponding to the azimuthal angles of 0.34° and
392 359.6° , respectively. The ordinate is the gate number from 1 to 800, equivalent to the
393 one nearest to the radar and the maximum range, respectively. Warm (cold) colors
394 represent the target motion toward (away from) the radar. The range gates without
395 observations are represented in black. (b) As in Fig. 2a, but for the velocity field after
396 quality control is performed by the proposed algorithm.

397

398 Figure 3: (a) As in Fig. 2a, but for the New Chitose radar data at 1740 JST at an elevation
399 angle of 32.1° . The observed velocities in this PPI scanning are confined to a limited
400 area, as indicated in this figure. The range of the abscissa (ordinate) is from 64 to 384
401 (from 15 to 140), and the respective azimuth (range) is from 44.3° to 269.3° (from 2.25
402 km to 21 km). (b) As in Fig. 3a, but for the corrected field.

403

404 Figure 4: (a) As in Fig. 2a, but for the Ushio radar data at 1801 JST at an elevation angle
405 of 4.9°. Data are shown up to the gate number of 500, beyond which no data were
406 observed. The beam number 1 corresponds to 0.60°, and the beam number 300
407 corresponds to 359.4°. Erroneous data are present in regions enclosed by yellow lines.
408 The velocity data in the green rectangle are enlarged in Fig. 4b. An enlarged view of a
409 portion enclosed in the bright magenta frame is also displayed in the mini-window of red
410 frame to clearly show erroneous data located in a yellow circle. This mini-window is
411 placed in a portion without observed data. For these two frames, the left and right
412 sides correspond to the beam number of 190 and 210, respectively, while the bottom
413 and top sides correspond to the gate number of 275 and 295, respectively. Note that
414 the aspect ratio differs between these frames. (b) Enlarged view of velocity data
415 clipped from the region in the green rectangle in Fig. 4a. Errors and/or noise are
416 enclosed by a circle and oval in yellow. A pink rectangle indicates the window size
417 employed for the gap check process. (c) As in Fig. 4a, but for data after quality control is
418 performed by the present algorithm. (d) As in Fig. 4b, but for the data after correction.
419
420
421

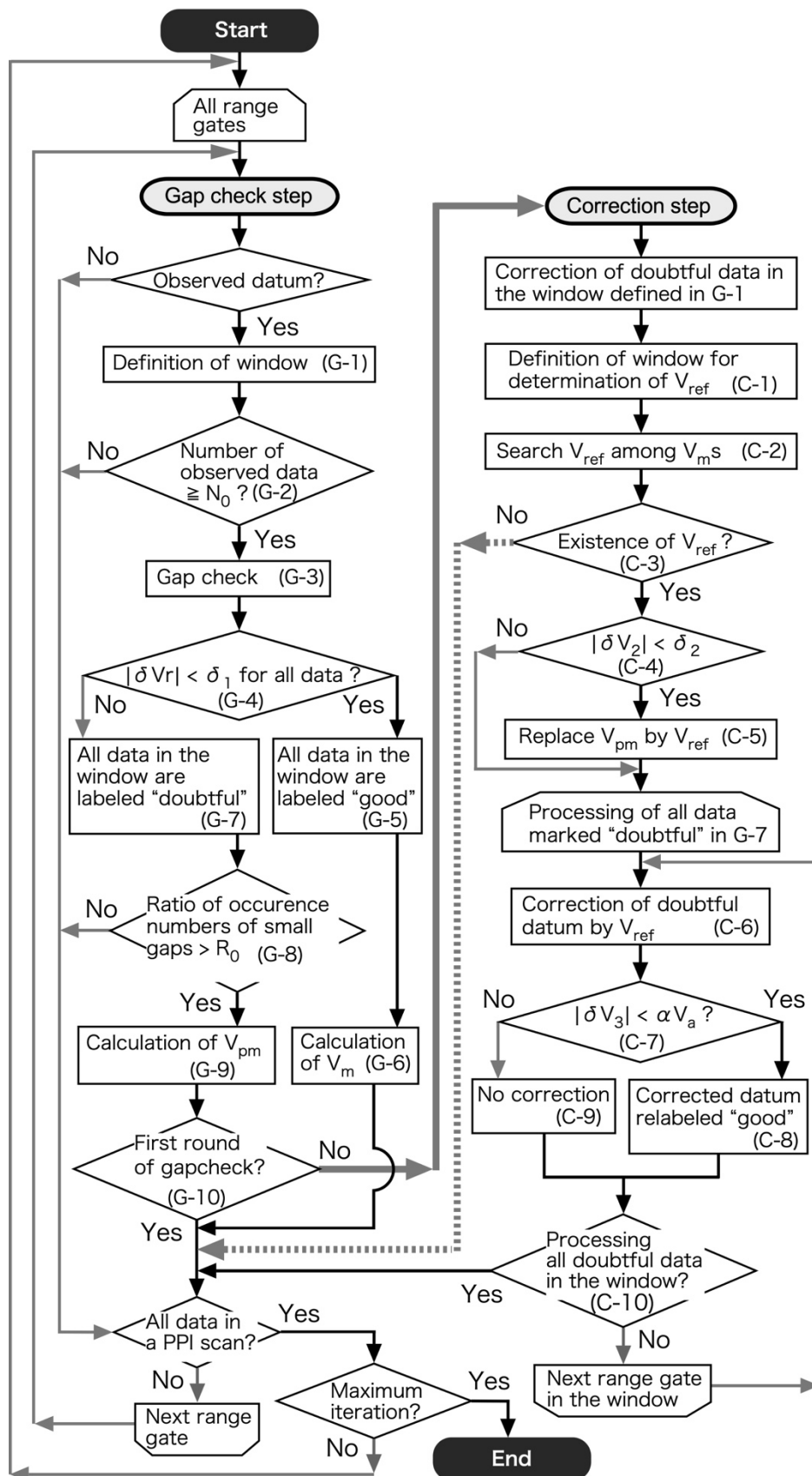


Fig. 1

422

423 Fig. 1 Flowchart of the proposed algorithm. The symbols in parentheses indicate important
 424 processes that are explained in the text.

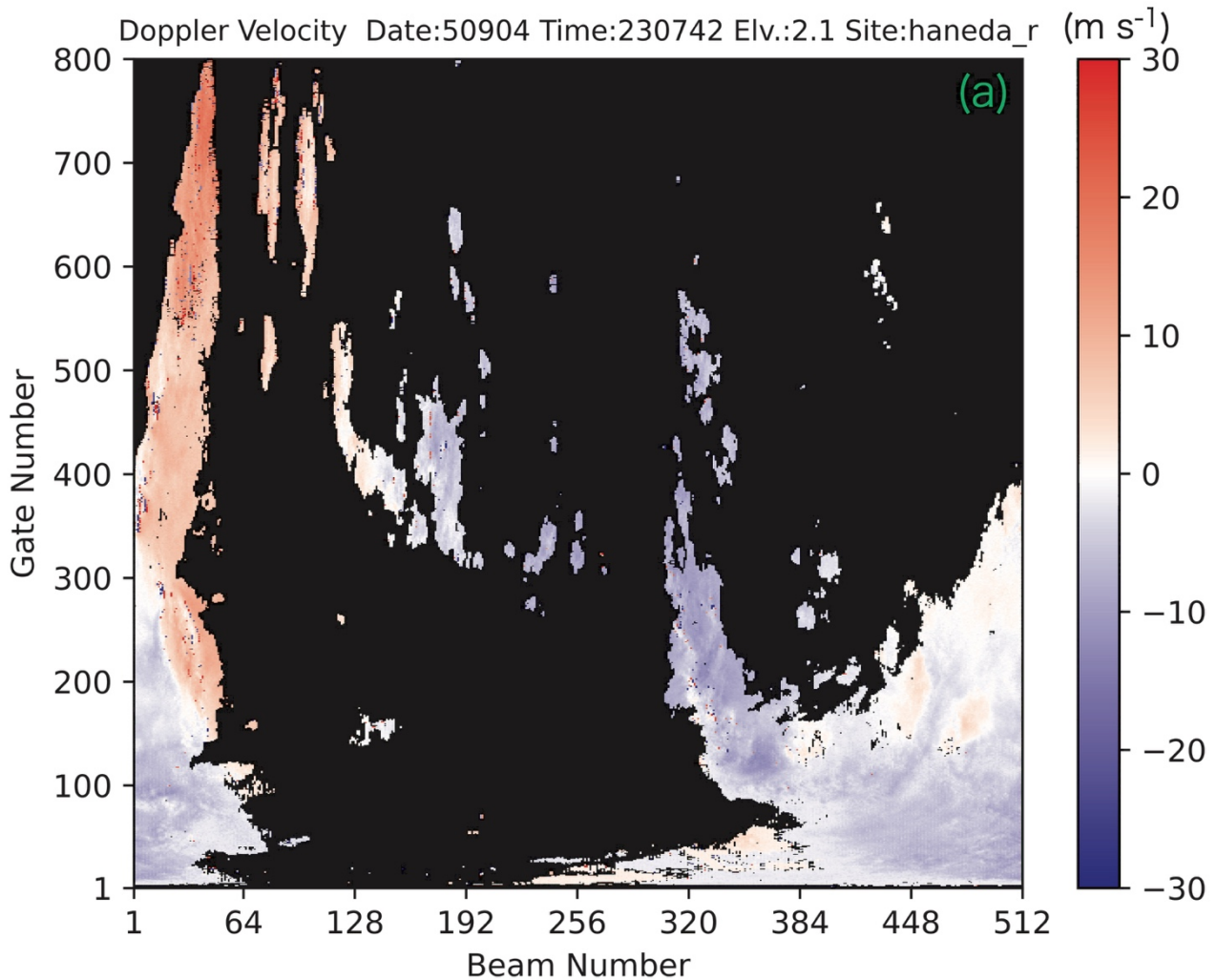


Fig. 2a

425

426

427 Fig. 2a: Beam-by-beam representation of Doppler velocity from the Haneda radar in a PPI

428 scan at an elevation angle of 2.1°. The abscissa indicates the beam number from 1 to

429 512 in a clockwise direction, corresponding to the azimuthal angles of 0.34° and 359.6°,

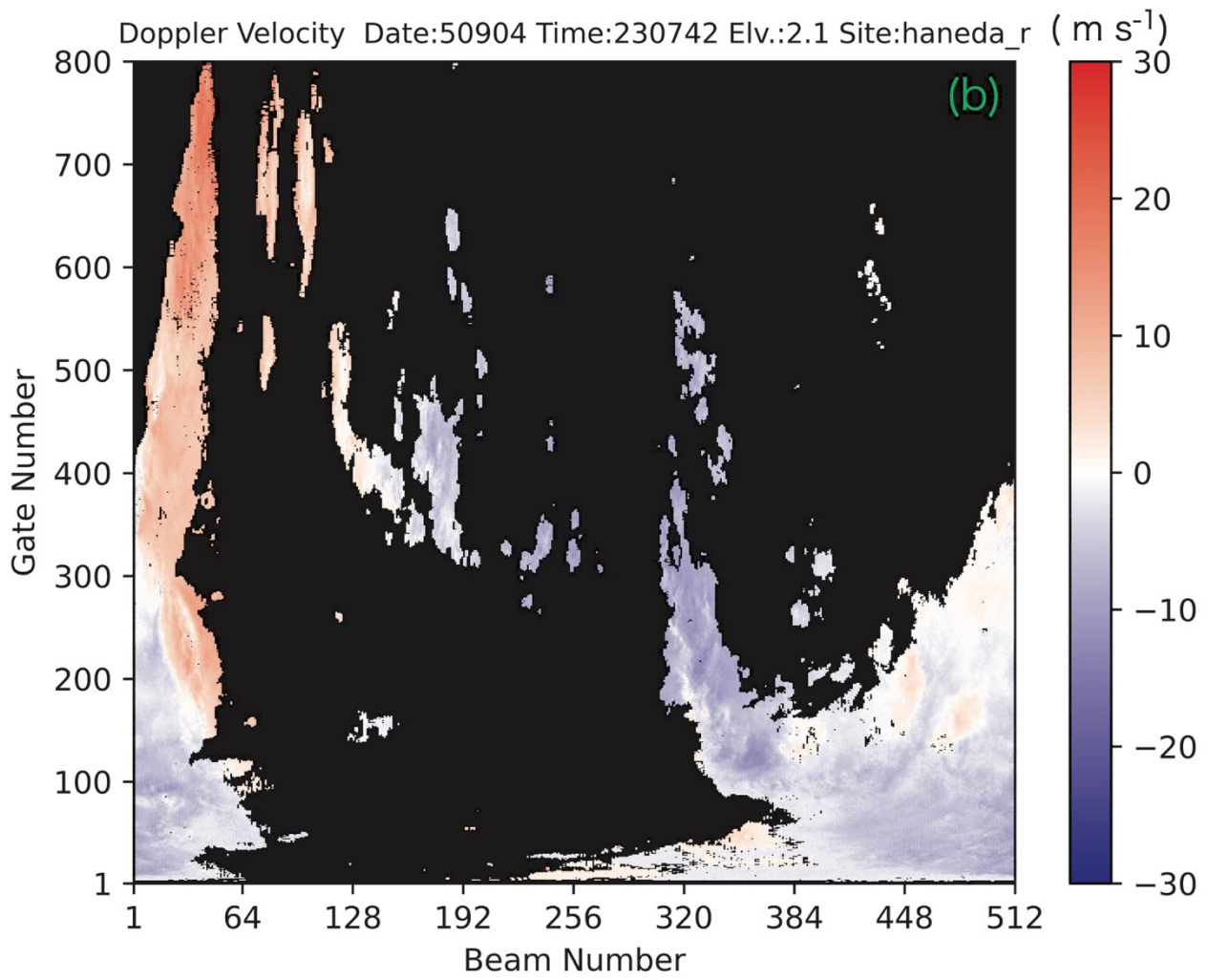
430 respectively. The ordinate is the gate number from 1 to 800, equivalent to the one

431 nearest to the radar and the maximum range, respectively. Warm (cold) colors

432 represent the target motion toward (away from) the radar. The range gates without

433 observations are represented in black.

434



435

Fig. 2b

436

437 Fig. 2b: As in Fig. 2a, but for the velocity field after quality control is performed by the

438 proposed algorithm.

439

440

441

442

443

444

445

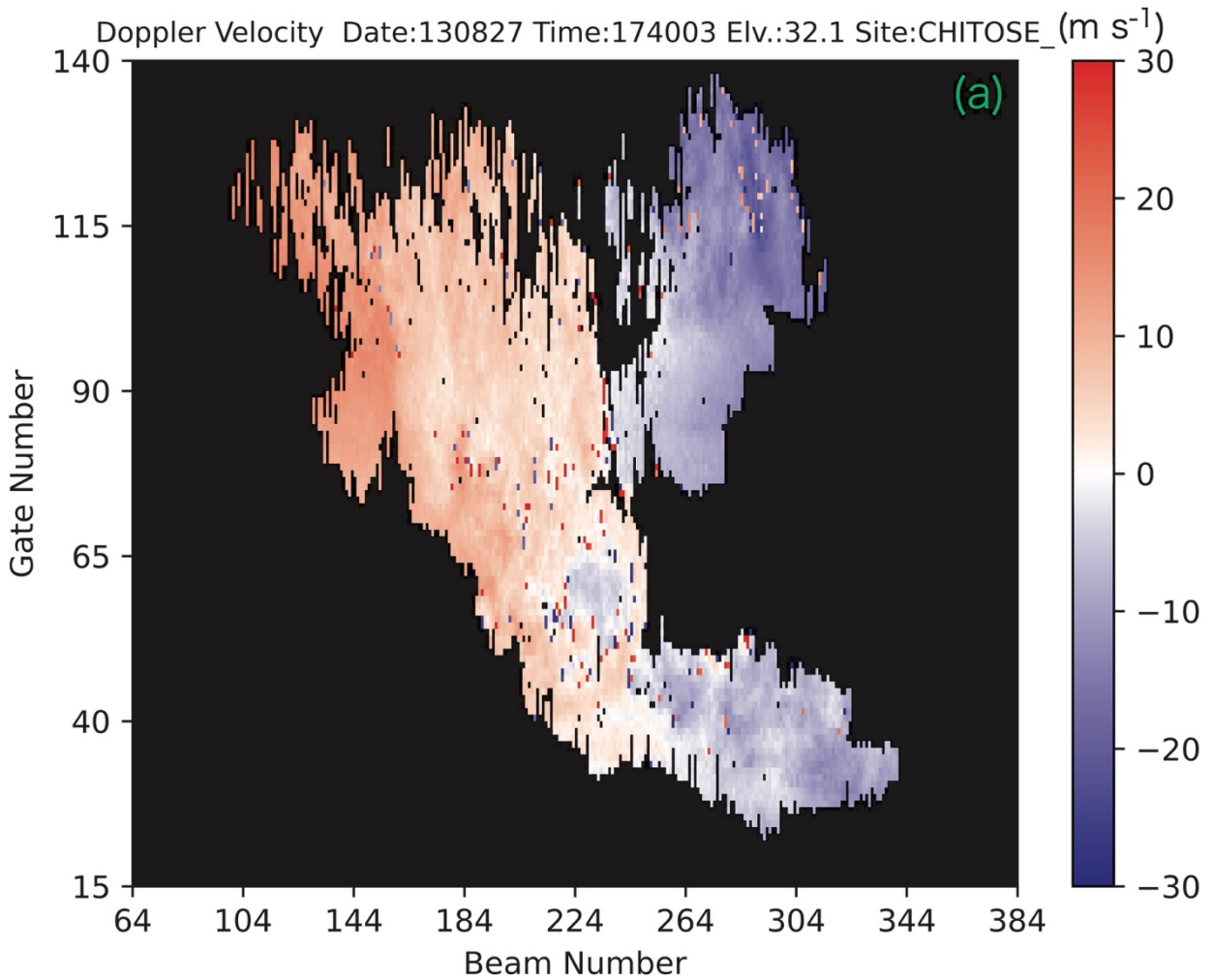


Fig. 3a

446

447 Fig. 3a: As in Fig. 2a, but for the New Chitose radar data at 1740 JST at an elevation angle
 448 of 32.1° . The observed velocities in this PPI scanning are confined to a limited area,
 449 as indicated in this figure. The range of the abscissa (ordinate) is from 64 to 384 (from
 450 15 to 140), and the respective azimuth (range) is from 44.3° to 269.3° (from 2.25 km to
 451 21 km).

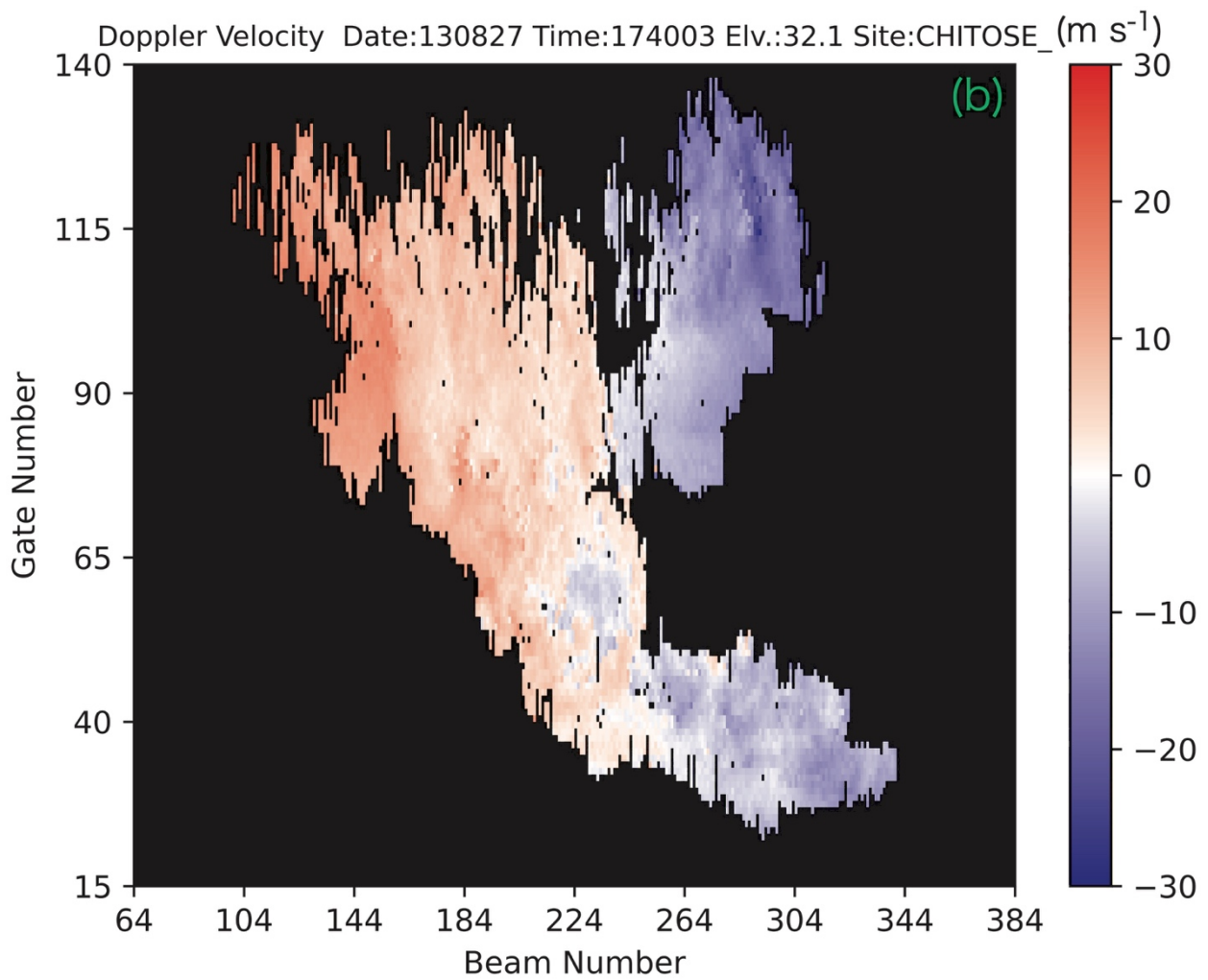
452

453

454

455

456



457

Fig. 3b

458 Fig. 3b: As in Fig. 3a, but for the corrected field.

459

460

461

462

463

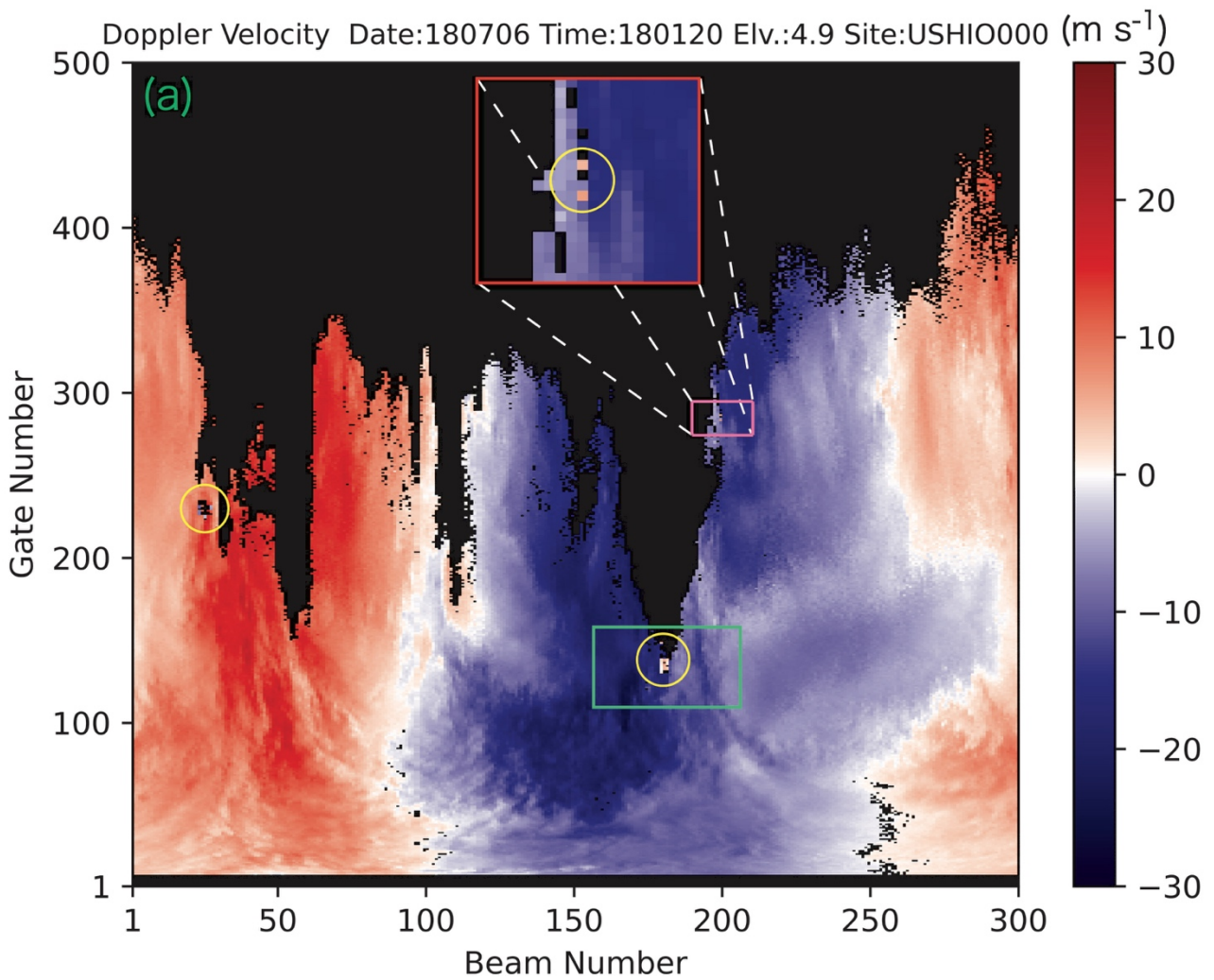
464

465

466

467

468



469

Fig. 4a

470

471

Fig. 4a: As in Fig. 2a, but for the Ushio radar data at 1801 JST at an elevation angle of

472

4.9°. Data are shown up to the gate number of 500, beyond which no data were

473

observed. The beam number 1 corresponds to 0.60° , and the beam number 300

474

corresponds to 359.4° . Erroneous data are present in regions enclosed by yellow

475

circles. The velocity data in the green rectangle are enlarged in Fig. 4b. An enlarged

476

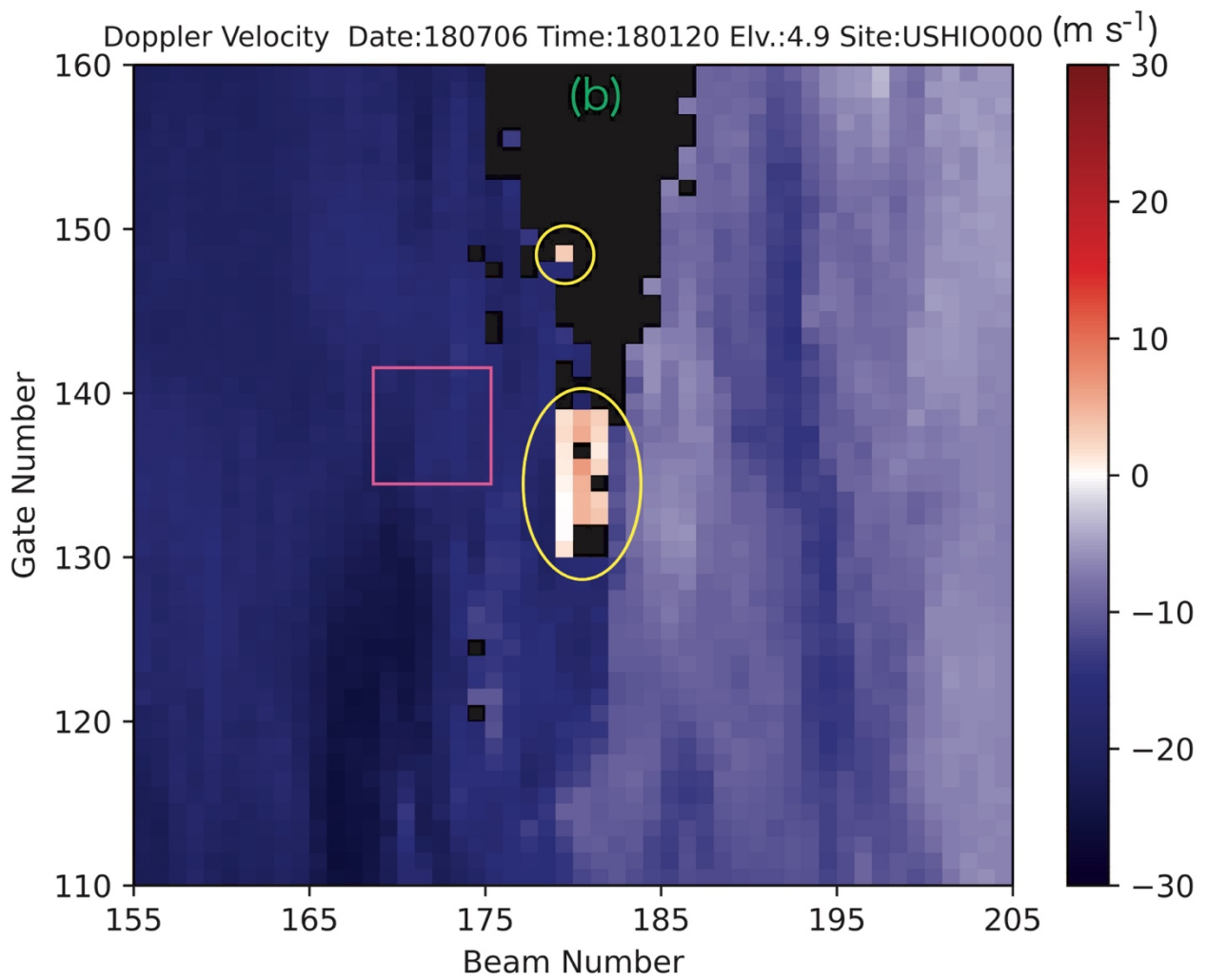
view of a portion enclosed in the bright magenta frame is also displayed in the mini-

477

window of red frame to clearly show erroneous data located in a yellow circle. This

478 mini-window is placed in a portion without observed data. For these two frames, the
479 left and right sides correspond to the beam number of 190 and 210, respectively, while
480 the bottom and top sides correspond to the gate number of 275 and 295, respectively.
481 Note that the aspect ratio differs between these frames.

482



483

Fig. 4b

484

485 Fig. 4b: Enlarged view of velocity data clipped from the region in the green rectangle in
 486 Fig. 4a. Errors and/or noises are enclosed by a circle and oval in yellow. A pink
 487 rectangle indicates the window size employed for the gap check process.

488

489

490

491

492

493

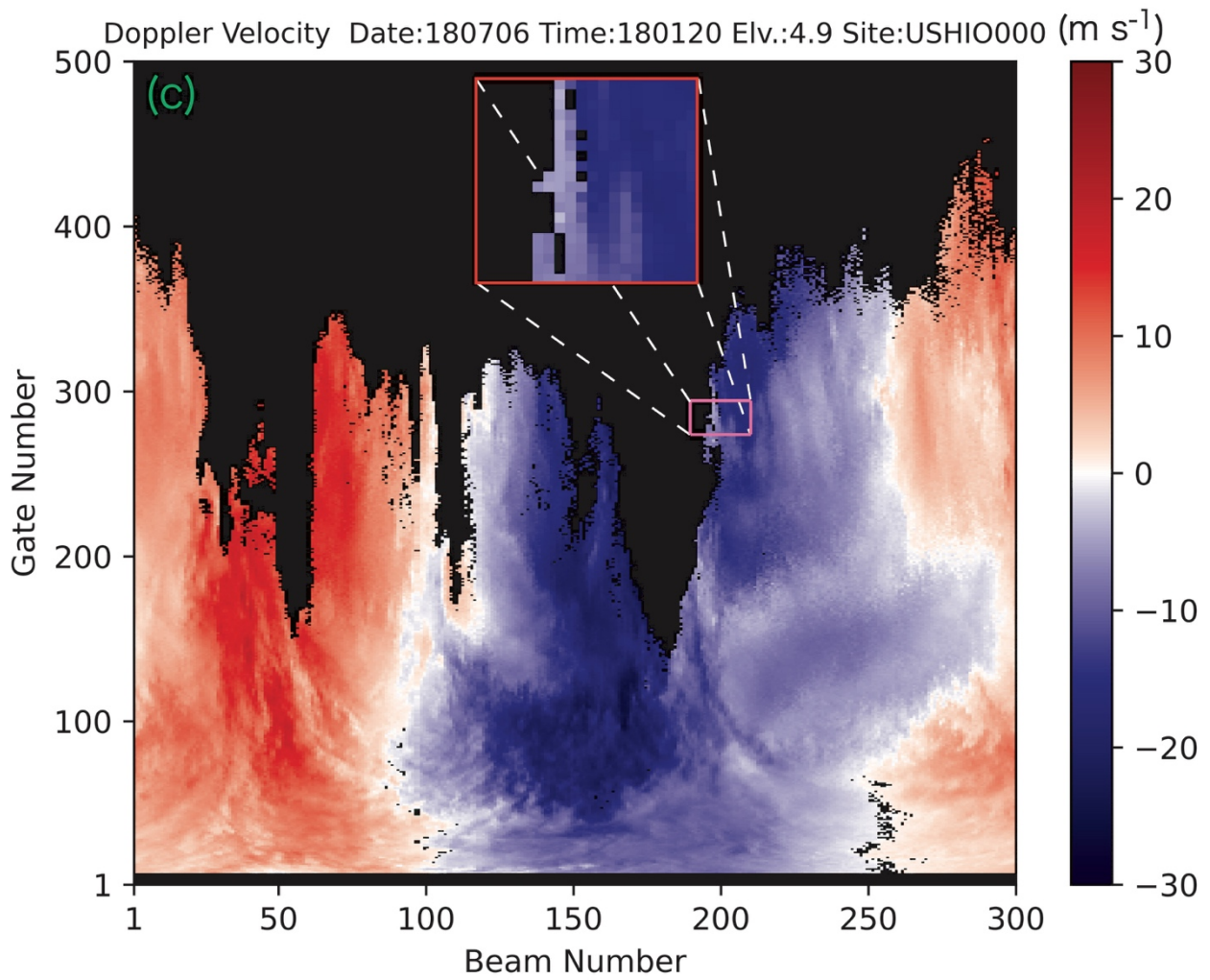
494

495

496

497

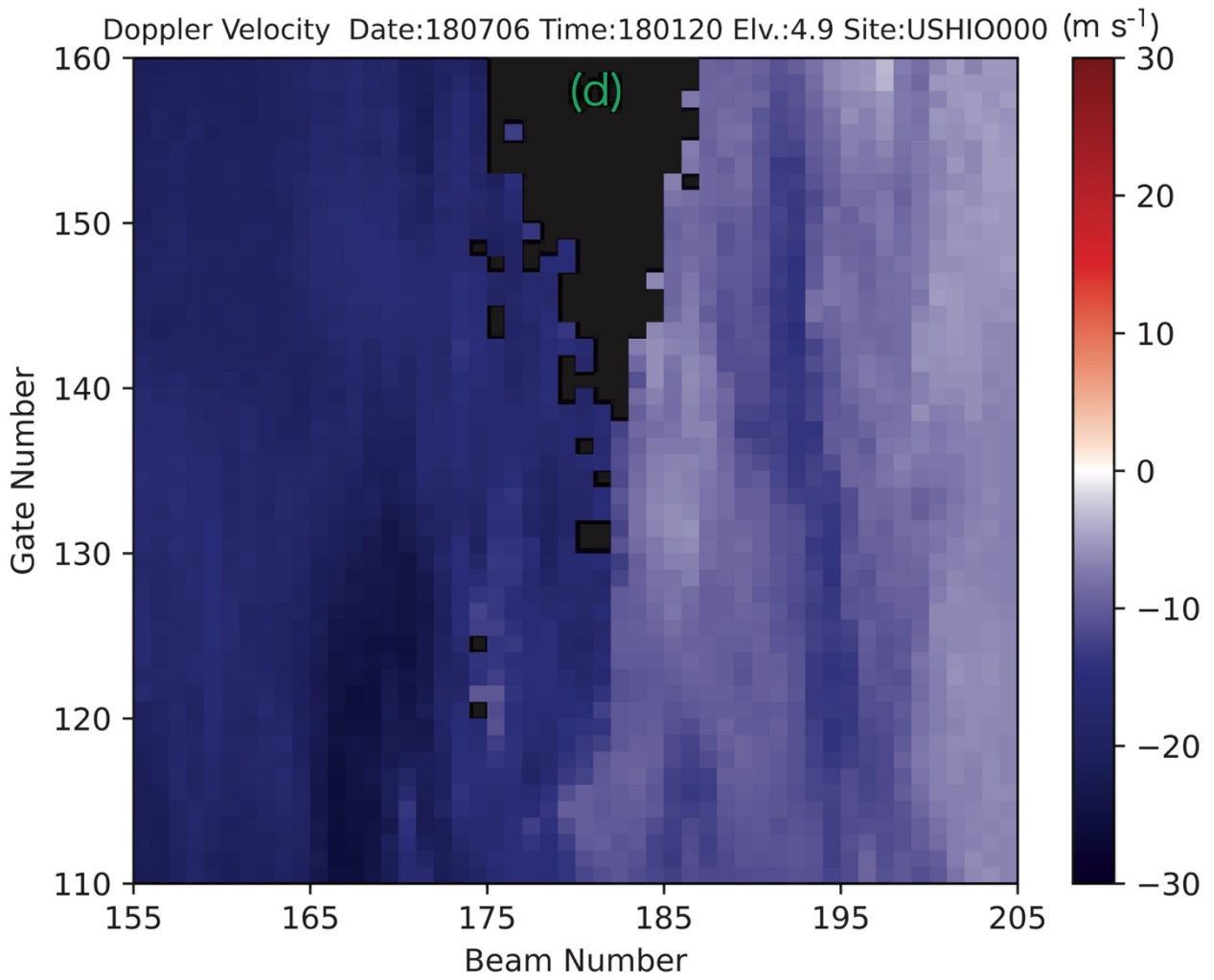
498



499
 500
 501
 502
 503
 504

Fig. 4c

Fig. 4c: As in Fig. 4a, but for data after quality control is performed by the present algorithm.



505

Fig. 4d

506 Fig. 4d: As in Fig. 4b, but for the data after correction.

507

508

509

510

511

512

513